IEEE Photonics Journal
An IEEE Photonics Society Publication

High-Performance Silicon 2 × 2 Thermo-Optic Switch for the 2-μm Wavelength Band

Volume 11, Number 4, August 2019

Li Shen
Meng Huang
Shuang Zheng
Lesi Yang
Xiangfeng Peng
Xiaoping Cao
Shuhui Li
Jian Wang

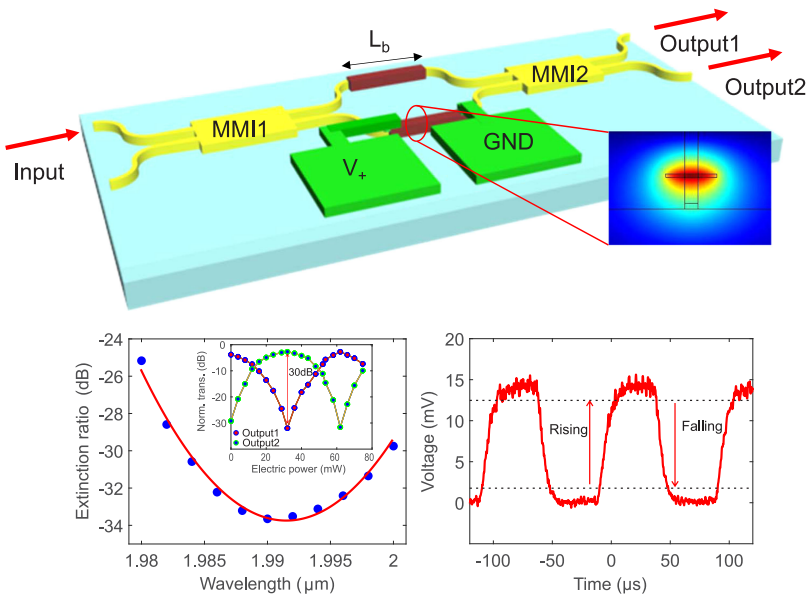

DOI: 10.1109/JPHOT.2019.2921923

High-Performance Silicon 2 × 2 Thermo-Optic Switch for the 2-μm Wavelength Band

Li Shen, Meng Huang, Shuang Zheng, Lesi Yang, Xiangfeng Peng, Xiaoping Cao, Shuhui Li, and Jian Wang

Wuhan National Laboratory for Optoelectronics, School of Optical and Electronic Information, Huazhong University of Science and Technology, Wuhan 430074, China

DOI:10.1109/JPHOT.2019.2921923

Manuscript received April 26, 2019; revised May 30, 2019; accepted June 6, 2019. Date of publication June 10, 2019; date of current version July 16, 2019. This work was supported in part by the Natural Science Foundation of China under Grants 61705072, 61761130082, 11574001, 11774116, 11274131, and 61222502, in part by the Royal Society-Newton Advanced Fellowship, in part by the Natural Science Foundation of Hubei province (ZRMS2017000413), in part by the National Basic Research Program of China (973 Program) (2014CB340004), in part by the National Program for Support of Top-notch Young Professionals, and in part by the Program for HUST Academic Frontier Youth Team. Corresponding author: Jian Wang (e-mail: jwang@hust.edu.cn).

Abstract: The 2-μm spectral window is emerging as a promising candidate for the next generation communication. We present a 2 × 2 Mach–Zehnder interferometric thermo-optic switch at 2-μm waveband. The device is fabricated on a 220 nm thick silicon-on-insulator wafer with standard complementary metal oxide semiconductor (CMOS) process. We demonstrate an over 30 dB extinction ratio under the power consumption of 32.3 mW, with an average switching time of ~15 μs. This proof of principle optical switch paves a way toward full silicon-based chip-scale interconnects in the 2-μm waveband.

Index Terms: Optical interconnects, silicon photonics, 2-μm spectral window

1. Introduction

Recently, the 2-μm waveband is attracting increasing interests for expanding communications window to ease capacity issues as the current standard single-mode fibers (SMFs) based near infrared telecommunication network is approaching its theoretical limit [1]. In the meantime, active optical fibers (e.g. thulium- or holmium-doped fibers (TDF/HDF)) can provide a high and broadband gain window at the two micron spectral band outside the traditional 1550 nm telecom band [2], [3]. Over the past few years, the developments in the 2-μm band including high-performance laser sources [4], [5], broad bandwidth amplifier [6], high-speed optical modulators [7] and photodetector [8], and the benchmark low-loss hollow-core photonic bandgap fibers (HC-PBGFs) [9], have enabled a wide range of applications not only for telecom [10], but also for sensing and biomedical monitoring [11].

Among these well-established technologies, the integrated complementary metal oxide semiconductor (CMOS) compatible photonic platform like silicon-on-insulator (SOI) could be the preferred solution as its advantages such as high volume, small footprint, and low cost fabrication still exist for this new wavelength band. Furthermore, the advanced LIGO plans to employ 2-μm laser sources for the next generation of gravitational-wave detection, because of lower noise performance of its silicon test masses at this longer wavelength [12]. Owning to silicon's intrinsic optical

$$\Delta\phi = k \cdot \Delta n_{eff} \cdot L_h.$$

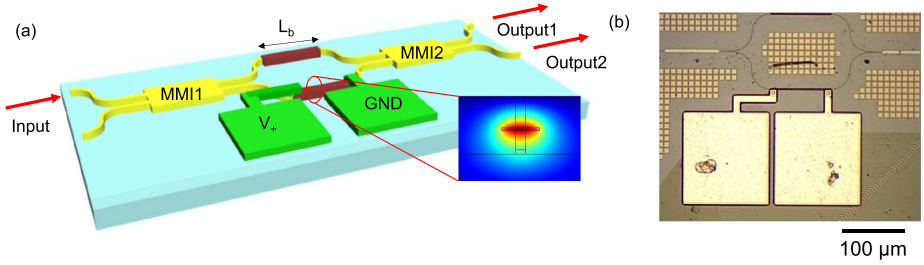

Fig. 1. (a) Schematic structure of the proposed optical switch. Inset: simulated heat distributions with the heater. (b) The optical image of the fabricated device.

transparency and negligible nonlinear absorption at the 2-μm wavelength, there are various recent demonstrations of integrated components including grating coupler [13], multimode interference (MMI) couplers [14], [15], and wavelength multiplexers [16], [17], which clearly shows the great potential of silicon devices to realize practical 2-μm systems. One of the realistic applications could be optical interconnect for intra/inter datacenter communications operating at the 2-μm waveband, as most of the basic optical components are currently available [18]. However, optical switches, one of the core building blocks for optical interconnects [19], have yet been demonstrated for this wavelength.

In this work, we for the first time design and fabricate an elegant silicon photonic switch at 2-μm waveband based on two multimode interferometers (MMIs) and a thermo-optic tunable phase shifter. The 2-μm optical switch was fabricated on the standard 220 nm thick SOI platform and thus is compatible with all the existing fabrication processes. In the experiments, we have measured large optical extinction ratio over 30 dB for $\sim$18 nm bandwidth. Furthermore, optical switching can be achieved with relatively low power consumption of 32.3 mW and fast switching time ($\sim$15 μs) has been measured at 2 μm. These results pave the way for the development of compact, low power, and integrated silicon optical switch devices for future 2-μm optical networks.

2. Concept

As shown in Fig. 1(a), the 2 × 2 optical switch device is based on a simple Mach-Zehnder interferometric (MZI) structure, where switching is achieved by inducing a π-phase shift to one of the interferometric arms. Two MMIs with the same optical path-length are used as 3-dB optical couplers for input and output connections. The operation principle can be simply described as follows: light is firstly injected from an input port of MMI1, and it is split into two arms of the MZI waveguides. A π-phase shift is induced to one arm of the MZI and then two light paths are combined by using a second MMI2. The output light can be chosen to pass through either output1 or output2 according to the corresponding switch mode. Bending waveguides (R = 30 μm) are introduced in the MMIs to increase the distance between the two arms for improved heat isolation. An analytical picture shows a typical heat distribution of the electrode in the inset of Fig. 1(a). The MZI based optical switches have been demonstrated with low-power consumption, fast response times, stable thermal performance and high fabrication tolerances at the near-infrared wavelengths, which are also expected for our devices designed for the 2-μm wave band [20]. Although the microring resonators (MRRs) usually exhibited a lower power consumption and smaller footprint [21], limited operation bandwidth and high temperature sensitivity will hinder its practical use for the optical switch.

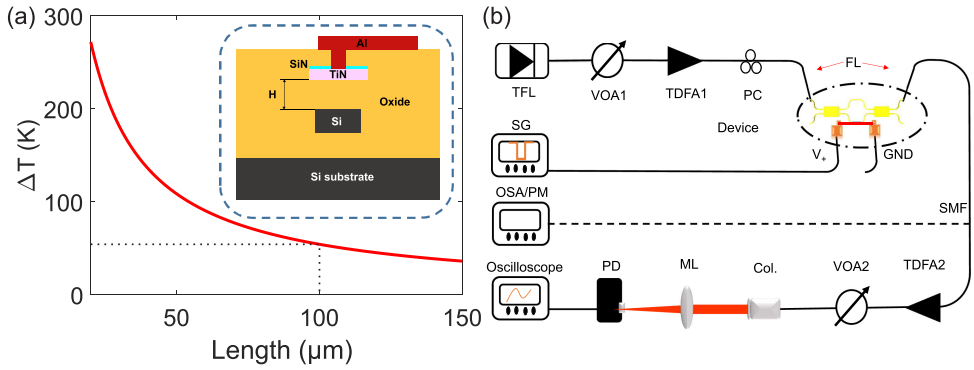

Fig. 2. (a) The relationship between L_h and ΔT in a TOPS. Inset: cross-section of waveguide and the heater. (b) Experimental set up. TFL: tunable laser; VOA: variable optical attenuator; TDFA: thulium-doped fiber amplifier; PC: polarization controller; SG: signal generator OL: objective lens; PD: photodetector; OSC: oscilloscope; PM: power meter.

3. Phase-Shifter Design and Device Fabrication

Thermo-optic phase-shifter (TOPS) is applied to one of the MZI arms to realize phase shift through heating the electrode above the silicon waveguide. In a TOPS, the relationship between phase $\Delta\phi$ and the effective index change can be estimated as:

$$\Delta\phi = k \cdot \Delta n_{\mathit{eff}} \cdot L_h. \tag{1}$$

Where L_h is the phase shifter length and $k = 2\pi/\lambda$ is the wavelength number. The effective index change Δn_{eff} can be calculated from the refractive index change Δn. Δn is determined by the thermal coefficient of the silicon material ($\partial n/\partial T$) and can be expressed as:

$$\Delta n = \frac{\partial n}{\partial T} \cdot \Delta T, \tag{2}$$

where the thermal coefficient for silicon is $1.84 \times 10^{-4}\,\mathrm{K}^{-1}$. We calculated the relationship between L_h and temperature change ΔT when a π-phase shift is achieved, and the results are shown in Fig. 2(a). It can be seen that ΔT remains almost constant when L_h is beyond 100 μm. Hence we choose 100 μm as the length of the heater and the arm waveguides to maintain a relatively small footprint.

The designed optical switch was fabricated at Institute of Microelectronics (IME), following the standard fabrication process on a SOI wafer with 220 nm top silicon and 2 μm buried oxide layer. The waveguides outlines were etched fully down 220 nm to the buried oxide. The top of the fabricated optical device was covered by a layer of 3 μm thick silica. Subsequently, contact holes were etched and a thin flat TiN heater was inserted above the MZI arm. The inset of Fig. 2(a) shows the cross-section of waveguide and the heater. The heater is located (H = 2 μm) above the silicon waveguide, thus resulting in negligible additional propagation loss. The width of heat resistance is 2 μm and the length is equal to that of the arm waveguide. Finally, two aluminium pads were applied to provide suitable voltage for the heater and were linked to the heater through two wells. Vertical grating couplers were fabricated for light coupling. The overall device footprint is 0.45 mm^2 including the electrodes.

4. Experimental Set Up and Results

Figure 2(b) shows the experiment set up for the 2-μm 2 × 2 optical switch. The light was coupled into and collected from the optical switch by using two grating couplers. The transmission of the grating coupler was measured by using a mid-IR supercontinuum source (OYSL SC-5-FC). An in-house built 2-μm tunable fiber laser (TFL) was used to charaterize the insertion loss of the whole device.

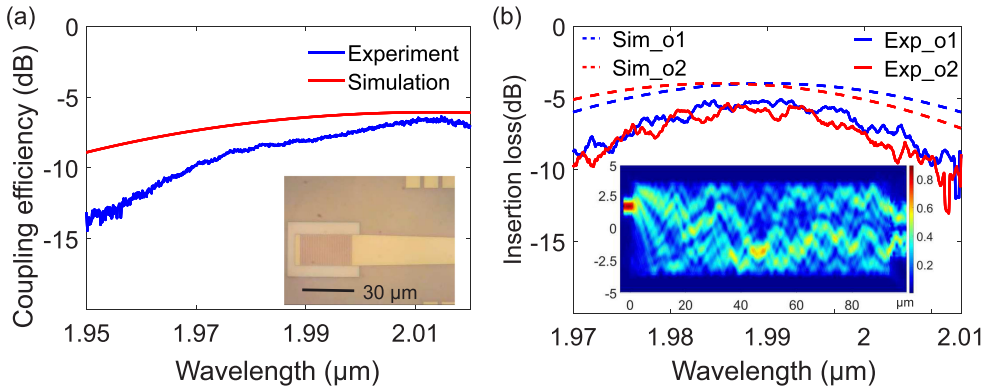

Fig. 3. (a) The simulated and measured coupling efficiency of the grating coupler. Inset: the microscope image of the grating coupler. (b) The simulated and the measured transmission of MMI. Inset: the numerically calculated electric fields.

The light was amplified by a high power thulium-doped fiber amplifier (TDFA1 AdValue Photonics AP-AMP-2000) and coupled into the waveguide with a vertical grating coupler. The voltage of the heater is changed through adjusting the voltage of the thermal probe. Two probe of the thermal heater are connected with the pattern of V+ and GND respectively. The output light was collected using another lens fiber from the chip. The output optical power of the two channels were recorded as a function of the driving power when changing the voltage applied to the electrodes. In addition to power consumption, the responding time of the device was characterized using the same setup, where the output temporal waveform was measured using a 2-μm high speed photodetector (PD, EOT ET-5000), capable of detecting 10 Gbps. A square electric wave was applied to the electrodes through a waveform generator. TDFA2 was used to amplify the output light before the PD and a VOA2 is used to adjust the amplified output for detection.

The grating couplers were designed with 16-degree tilt and 70 nm etching depth. The period of grating coupler is 926 nm, as shown from the inset of Fig. 3(a). The coupling efficiency curve is normalized and plotted in Fig. 3(a), together with the calculated coupling efficiency. The discrepancy between the measured insertion losses of the vertical grating couplers and the simulated coupling efficiency is probably due to an over-etching error occurred in the fabrication. We expect that the loss of the grating coupler could be improved by redesigning the etch depth and introducing complex apodized period, or increasing the thickness of silicon in the future optimization work.

The MMI was designed according to self-image theory. Numerically calculated electric fields in the MMI using the 3D Finite-Difference Time-Domain (FDTD) method is shown in the inset of Fig. 3(b). It can be seen that the power is almost distributed to the two ports equally using the following MMI parameters: the length, $L = 89.5$ μm and the width, $W = 6$ μm. The input and output of MMI are all tapered waveguides and the maximum width $W_a = 1.5$ μm and the minimum width are equal to the bending waveguide ($W_b = 0.65$ μm) for the fundamental mode condition. The length of this tapered waveguides $L_c = 20$ μm and the distance between the center of the tapered waveguide and the center of MMI is 1 μm. Figure 3(b) shows the measured insertion losses of the two ports. The insertion loss of the two ports is nearly equal between 1.97 to 2.01 μm. The minimum extra losses (2 dB) introduced by the MMI occur roughly in 1.99 μm and the 3 dB bandwidth is over 30 nm.

The maximum extinction ratio with applied electric power was measured as a function of wavelength using the 2-μm tunable laser and the power meter. As it can be clearly seen from Figure 4(a), the maximum extinction ratio is $\sim$33.5 dB at its designed wavelength (1.99 μm). The 3 dB operation bandwidth is over 18 nm, which is much broader than MRR based optical switches as expected [7], [13]. The characterizations of power consumption at maximum extinction ratio and switching speed were subsequently performed using a single laser source with at a fixed wavelength of 2 μm. For power consumption measurement, the applied electric power was scanned from 0 to 75 mW and

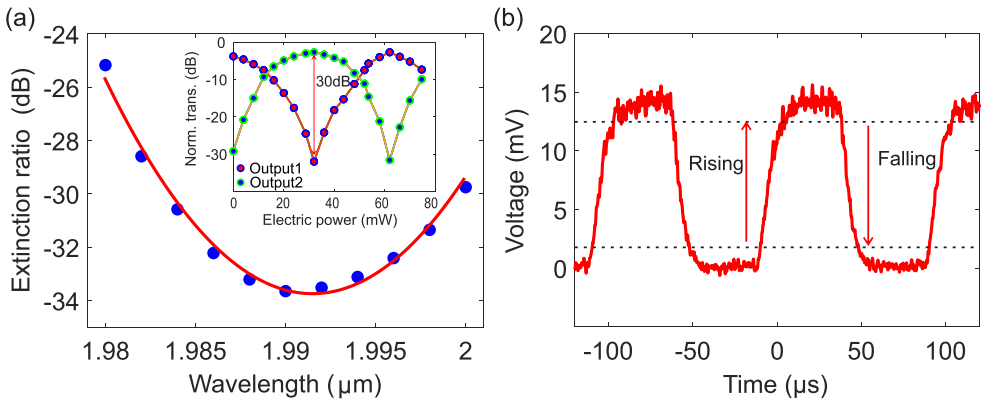

Fig. 4. (a) Maximum extinction ratio as a function of wavelength. Inset: Normalized transmission as a function of the applied electric power measured at 2 μm. (b) Optical switching responding time.

TABLE 1
Performance of MZI Thermo-Optic Switches

Footprint (mm^2)	Power consumption (mW)	Optical loss (dB)	Extinction ratio (dB)	Switching speed (μs)	Wavelength (μm)	Year [Ref.]
0.49	40	4	50	30	1.55	2010 [23]
0.005^*	24.9	2	~32	1.19	1.55	2016 [22]
-	47	1.3-2.2	30.5	-	3.8	2014 [24]
0.45	32.3	2-3	30	15	2.0	This work

*Electrodes is not included in the device footprint.

the output optical power was recorded at the same time. The inset of Figure 4(a) shows the normalized output power of the optical switch at both output ports as a function of the applied electric power. It can be seen that optical switch from output1 to output2 can be achieved at a relatively low electric power of 32.3 mW. Namely, a π-phase shift has been realized. With a power of 60.5 mW, a 2π-phase shift can be achieved. When the switch power is 32.3 mW (corresponding to V+ = 4.1 V), the extinction ratio between the two ports reach ~30 dB. The few Volts drive voltage requirement used in our experiments is easily attainable using conventional cost-effective electrical drivers. It could be further reduced by optimising the electrodes design, following similar approaches applied in the near infrared optical switches [22]. It is worth noting that a 33.5 dB extinction ratio is among the largest values reporting for a single MZI. This extinction ratio could be improved to at least 50 dB by cascading an MZI array [23], as well as requiring reducing the losses of the element MZI waveguides to around 1 dB/cm or less.

For thermo-optic switch, the speed is mainly limited by relatively slow thermo-optic effects, and thus the switching time is usually at microsecond scale. A 10 kHz square-wave voltage signal, with a peak-to-peak voltage 4.1 V (for maximum extinction ratio) was applied to switch device. The optical waveform, measured by the high-speed detector, are showed in Fig. 4(b). The rising time (10% ~ 90%) and falling time (90% ~ 10%) of electrical signal, demonstrate an average switching time of ~15 μs for our 2-μm optical switch. Table 1 summarizes the performance of various typical MZI thermo-optic switches based on SOI waveguides. Our proof-of-concept 2-μm optical switch shows the comparable performance in terms of footprint, extinction ratio, power consumption, and switching speed with their mature counterparts at the well-developed near infrared wavelengths. It is worth noting that straight-arm MZI optical switch has also been demonstrated for longer mid-infrared wavelength at 3.8 μm with similar extinction ratio but requiring greater switching power of 245 mW [24]. Although the 2-μm optical switch can now be implemented by using the designed device mentioned above, its optical performance is largely constrained by the slightly higher transmission loss. The switch performance needs to be further improved reducing the insertion losses to around

1 dB and less by optimizing the MMI design and fabrication process. Furthermore, the coupling efficiency could also be enhanced by employing more efficient grating or edge coupling via inverse tapers.

5. Conclusion

In this paper, we design, fabricate and characterize a high performance thermo-optic tunable optical switch operating in emerging 2-μm communication window based on the standard platform of SOI (220 nm). The maximum extinction ratio of the optical switch is nearly 33.5 dB. At 2 μm, optical switching can be achieved with a low driving power of 32.3 mV. Fast switching time is measured to be $\sim$15 μs. All these results suggest this optical switch has various potential applications for on-chip optical interconnections in 2-μm waveband and it is compatible with other integrated devices of the tradition communication bands.

References

[1] D. J. Richardson, "Filling the light pipe," *Science*, vol. 330, no. 6002, pp. 327–328, 2010.
[2] Z. Li, A. M. Heidt, J. M. O. Daniel, Y. Jung, S. U. Alam, and D. J. Richardson, "Thulium-doped fiber amplifier for optical communications at 2 μm," *Opt. Exp.*, vol. 21, no. 8, pp. 9289–9297, 2013.
[3] F. C. Garcia Gunning, N. Kavanagh, E. Russell, R. Sheehan, J. O'Callaghan, and B. Corbett, "Key enabling technologies for optical communications at 2000 nm," *Appl. Opt.*, vol. 57, no. 22, pp. E64–E70, 2018.
[4] R. Phelan, J. O'Carroll, D. Byrne, C. Herbert, J. Somers, and B. Kelly, "$In_{0.75}Ga_{0.25}$ As/InP multiple quantum-well discrete-mode laser diode emitting at 2 μm," *IEEE Photon. Technol. Lett.* vol. 24, no. 8, pp. 652–654, Apr. 2012.
[5] S. Latkowski *et al.*, "Monolithically integrated widely tunable laser source operating at 2 μm," *Optica*, vol. 3, no. 12, pp. 1412–1417, 2016.
[6] Z. Li *et al.*, "Diode-pumped wideband thulium-doped fiber amplifiers for optical communications in the 1800-2050 nm window," *Opt. Exp.*, vol. 21, no. 22, pp. 26450–26455, 2013.
[7] W. Cao *et al.*, "High-speed silicon modulators for the 2-μm wavelength band," *Optica*, vol. 5, no. 9, pp. 1055–1062, 2016.
[8] J. J. Ackert *et al.*, "High-speed detection at two micrometres with monolithic silicon photodiodes," *Nature Photon.*, vol. 9, no. 5, pp. 393–396, 2015.
[9] Z. Liu *et al.*, "High-capacity directly modulated optical transmitter for 2 μm spectral region," *J. Lightw. Technol.*, vol. 33, no. 7, pp. 1373–1379, Apr. 2015.
[10] K. Xu, Q. Wu, Y. Xie, M. Tang, S. Fu, and D. Liu, "High speed single-wavelength modulation and transmission at 2 μm under bandwidth-constrained condition," *Opt. Exp.*, vol. 25, no. 4, pp. 4528–4534, 2017.
[11] A. Parriaux, K. Hammani, and G. Millot, "Two-micron all-fibered dual-comb spectrometer based on electro-optic modulators and wavelength conversion," *Commun. Phys.*, vol. 1, no. 17, pp. 1–7, 2018.
[12] S. Wills, "Gravitational waves: The road ahead," *Opt. Photon. News*, vol. 29, no. 5, pp. 44–51, 2018.
[13] J. Li *et al.*, "2-μm wavelength grating coupler, bent waveguide, and tunable microring on silicon photonic MPW," *IEEE. Photon. Technol. Lett.*, vol. 30, no. 5, pp. 471–474, Mar. 2018.
[14] M.-S. Rouifed *et al.*, "Low loss SOI waveguides and MMIs at the MIR wavelength of 2 μm," *IEEE. Photon. Technol. Lett.*, vol. 28, no. 24, pp. 2827–2829, Dec. 2016.
[15] H. Xie *et al.*, "Inversely designed 1 x 4 power splitter with arbitrary ratios at 2-μm spectral band," *IEEE. Photon. J.*, vol. 10, no. 4, Aug. 2018, Art. no. 2700506.
[16] M.-S. Rouifed *et al.*, "Ultra-compact MMI-based beam splitter demultiplexer for the NIR/MIR wavelengths of 1.55 μm and 2 μm," *Opt. Exp.*, vol. 25, no. 20, pp. 10893–10900, 2017.
[17] E. J. Stanton, N. Volet, and J. E. Bowers, "Silicon arrayed waveguide gratings at 2.0-μm wavelength characterized with an on-chip resonator," *Opt. Lett.*, vol. 43, no. 5, pp. 1135–1138, 2018.
[18] D. Miller, "Device requirements for optical interconnects to silicon chips," *Proc. IEEE*, vol. 97, no. 7, pp. 1166–1185, Jul. 2009.
[19] H. Subbaraman *et al.*, "Recent advances in silicon-based passive and active optical interconnects," *Opt. Exp.*, vol. 23, no. 3, pp. 2487–2510, 2015.
[20] N. Xie, T. Hashimoto, and K. Utaka, "Design and performance of low-power, high speed, polarization-independent and wideband polymer buried-channel waveguide thermo-optic switches," *J. Lightw. Technol.*, vol. 32, no. 17, pp. 3067–3073, Sep. 2014.
[21] N. Dupuis *et al.*, "Design and fabrication of low-insertion-loss and low-crosstalk broadband 2 × 2 Mach–Zehnder silicon photonic switches," *J. Lightw. Technol.*, vol. 33, no. 17, pp. 3597–3606, Sep. 2015.
[22] A. Rosa, A. Gutierrez, A. Brimont, A. Griol, and P. Sanchis, "High performace silicon 2 × 2 optical switch based on a thermos-optically tunable multimode interfence coupler and efficient electrodes," *Opt. Exp.*, vol. 24, no. 1, pp. 191–198, 2016.
[23] Y. Shoji, K. Kintaka, S. Suda, H. Kawashima, T. Hasama, and H. Ishikawa, "Low-crosstalk 2 × 2 thermo-optic switch with silicon wire waveguides," *Opt. Exp.*, vol. 18, no. 9, pp. 9071–9075, 2010.
[24] M. Nedeljkovic *et al.*, "Mid-infrared thermo-optic modulators in SOI," *IEEE. Photon. Technol. Lett.*, vol. 26, no. 13, pp. 1352–1355, Jul. 2014.